Calculation of the pK_a Values for the Ligands and Side Chains of *Escherichia coli* D-Alanine:D-Alanine Ligase

Heather A. Carlson,* James M. Briggs, and J. Andrew McCammon

Departments of Chemistry and Biochemistry and of Pharmacology, University of California, San Diego, La Jolla, California 92093-0365

Received June 8, 1998

Poisson−Boltzmann electrostatics methods have been used to calculate the pK_a shifts for the ligands and titratable side chains of D-alanine:D-alanine ligase of the *ddlb* gene of *Escherichia coli* (DdlB). The focus of this study is to determine the ionization state of the second D-alanine (D-Ala$_2$) in the active site of DdlB. The pK_a of the amine is shifted over 5 pK_a units more alkaline in the protein, clearly implying that D-Ala$_2$ is bound to DdlB in its zwitterionic state and not in the free-base form as had been previously suggested. Comparisons are made to the depsipeptide ligase from the vancomycin-resistance cascade, VanA. It is suggested that VanA has different enzymatic properties due to a change in binding specificity rather than altered catalytic behavior and that the specificity of binding D-lactate over D-Ala$_2$ may arise from the difference in ionization characteristics of the ligands.

Introduction

The D-alanine:D-alanine ligase of the *ddlb* gene of *Escherichia coli* (DdlB) is an ATP-dependent enzyme that promotes dipeptide formation of D-Ala-D-Ala.[1,2] D-Ala-D-Ala is then incorporated into a UDP-muramyl pentapeptide. The bactoprenyl cycle completes the UDP-muramyl pentapeptide into a disaccharide pentapeptide unit, *N*-acetylglucosamine-*N*-acetylmuramyl-L-Ala-D-Glu-*m*-diaminopimelic acid-D-Ala-D-Ala, and transports the unit through the membrane. The unit is then incorporated into the peptidoglycan polymer which gives the cell wall its tensile strength.[3,4] Within many prokaryotes, similar processes produce peptidoglycan polymers for the production of cell walls, and DdlB is similar to many other dipeptide ligases.[5] By understanding ligand binding in DdlB, modes of differentiation for dipeptide ligases can be elucidated. Inhibition of these processes could then be more accurately predicted and exploited as antibiotic targets.

The proposed mechanism of dipeptide ligation in DdlB is based on its crystal structure (Figure 1) and is given in Figure 2.[6] The first D-alanine (D-Ala$_1$) is bound and phosphorylated (phos-D-Ala$_1$) by ATP. The second D-alanine (D-Ala$_2$) is then bound, and the amine acts in a nucleophilic attack on the phosphoester of phos-D-Ala$_1$. The products of the reaction are ADP, an inorganic phosphate, and D-Ala-D-Ala.

There is some question regarding the ionization state of D-Ala$_2$. It has been proposed that D-Ala$_2$ may be in its free-base form, i.e., the anionic state, with a neutral amine and a carboxylate.[7] This has been proposed for several reasons. (1) The binding affinity of D-Ala$_2$ is approximately 1000-fold less than that of D-Ala$_1$ in DdlB, possibly indicating that the two substrates have different (electrostatic) characteristics. (2) The optimal pH for DdlB is 9.0.[8] Since the pK_a of the amine of D-Ala is 9.8,[9] approximately 10% of the D-alanine in solution will be present in the free-base form under optimal conditions. The 1000-fold reduction in binding of D-Ala$_2$ could arise from the need to scavenge the low population of the free-base form. (3) There is no obvious catalytic base present in the active site to deprotonate D-Ala$_2$. The ammonium must be deprotonated for the amine to act as a nucleophile in the dipeptide ligation. Originally, it was thought that Y216 may play this catalytic role, but the Y216F mutant of DdlB exhibits only a very slight decrease in catalytic efficiency (a free energy difference, ΔG_{cat}, of less than 0.2 kcal/mol between DdlB and its Y216F mutant).[8]

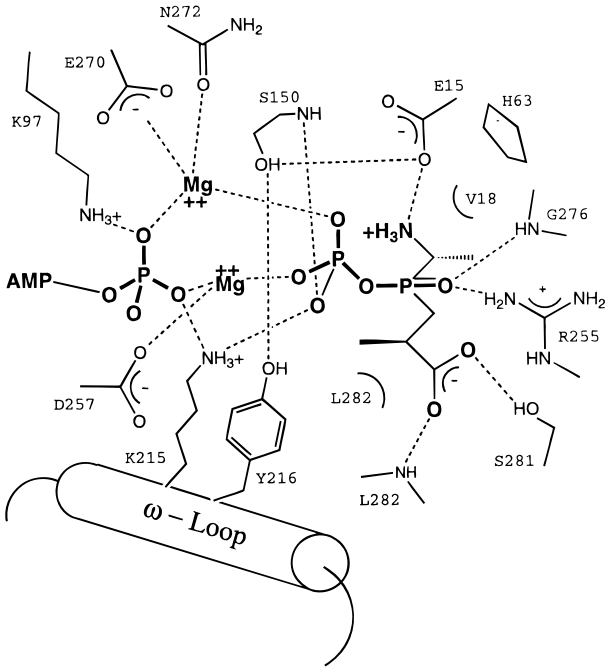

Figure 1. Schematic representation of the active site of DdlB with the phosphinophosphate transition-state mimic highlighted in bold.[6]

However, there are arguments against these points, as follows. (1) The difference in the affinity for D-Ala$_1$ and D-Ala$_2$ can be due to the fact that they do not have

10.1021/jm980351c CCC: $18.00
Published on Web 12/29/1998

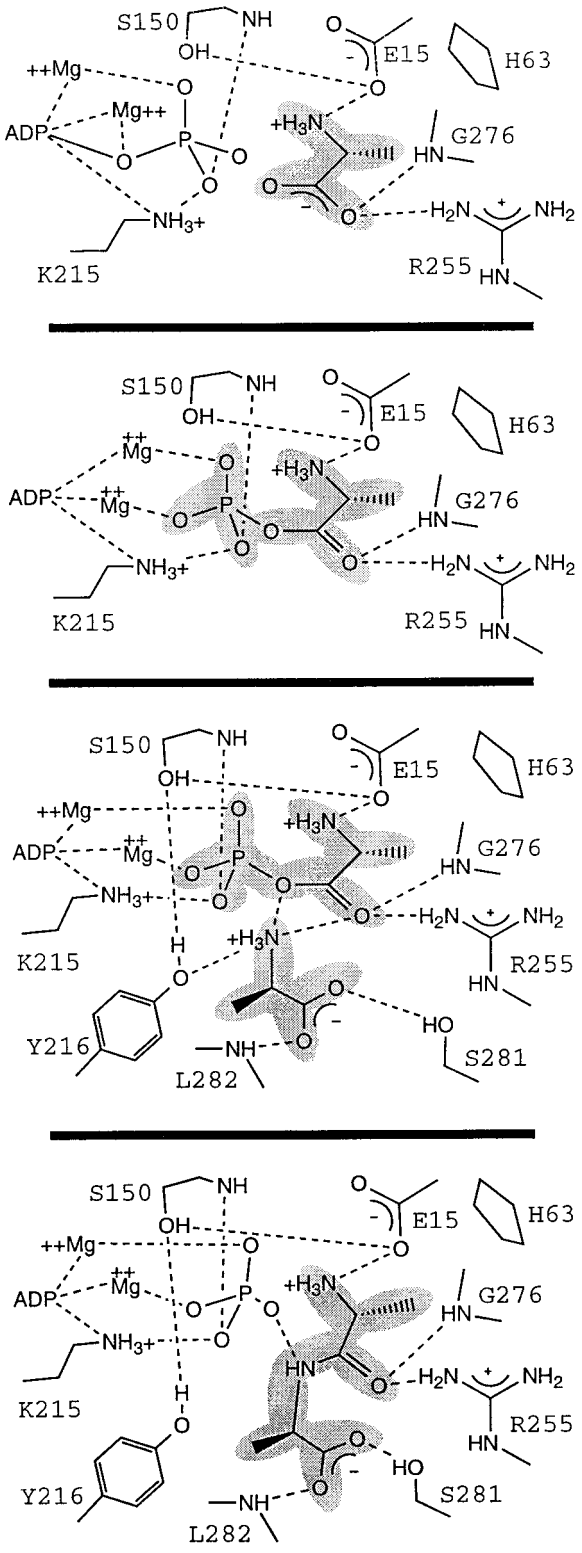

Figure 2. Binding and catalysis proposed for DdlB.[6,7] The ligands D-Ala_1, phos-D-Ala_1, and D-Ala_2 are highlighted with a gray background as well as the product, D-Ala-D-Ala. From the top, the schematics give the binding patterns of D-Ala_1, phos-D-Ala_1, D-Ala_2, and D-Ala-D-Ala with an inorganic phosphate ion.

the same interactions with active site residues. Notably, D-Ala_1 is complexed through charge complementarity to both the ammonium and carboxylate, and favorable charge interactions also complex D-Ala_1 after phosphorylation. The second active site does not provide charge complementarity to the carboxylate of D-Ala_2; instead the carboxylate accepts two hydrogen bonds from the hydroxyl group of S281 and the protein backbone; see Figure 2.

(2) In regard to the availability of a small population of free-base D-Ala_2, more recent studies have shown that the efficiency of DdlB, reported as $\log(k_{cat}/K_{m2})$, increases linearly from pH 6.0 to 9.5 but then decreases at pH 10.0 when the free-base form of D-Ala_2 becomes the dominant species in solution.[10] The authors of that study do not place much value on the decrease at pH 10 and interpret the linear trend to imply disfavored binding of D-Ala_2 at low pH where the zwitterionic species is dominant. If D-Ala_2 were to bind in the free-base form, K_{m2} from the experimental studies would definitely have a notable pH dependence, and $\log(k_{cat}/K_{m2})$ would be anticipated to increase by approximately 3 log units over pH 6.0 to 9.5 (see Appendix). However, the experimental data shows $\log(k_{cat}/K_{m2})$ to increase by only 1 log unit over that range. Because the linear trend seen in the experimental data differs by 2 orders of magnitude, the trend more likely points to slight changes in the protein environment with changing pH.

(3) The lack of change in k_{cat} for the Y216F mutant does not necessarily indicate that there is no deprotonation step. Differences in k_{cat} resulting from the mutagenesis of DdlB reflect the changes in the catalysis of the rate-limiting step. If the deprotonation of D-Ala_2 proceeds via Y216 but is not rate-limiting, there will be no change in k_{cat} for Y216F, providing that there is an alternative mechanism for losing the proton that is also faster than the rate-limiting step. Also, if the deprotonation step does not involve Y216, one would expect little change in any of the kinetic parameters. As k_{cat} is unaffected, it is not accurate to conclude whether Y216 or any other residue could be the catalytic base for deprotonation. It is also possible that a water molecule could act in this capacity since the crystal structure reveals two waters within hydrogen-bonding distance of the carboxylate of D-Ala_2.

Perhaps the strongest argument for D-Ala_2 to bind within DdlB in its zwitterionic form is the proximity of the amine to the phosphoester of phos-D-Ala_1. Being adjacent to a negatively charged functionality should promote the protonated form of the amine of D-Ala_2. However, the entire protein environment must be taken into account to accurately predict the charge state of D-Ala_2. To address the question of ionization states of the ligands and side chains of DdlB (most notably D-Ala_2), a "clustering method" employing Poisson–Boltzmann electrostatics has been used to determine the pK_a's and titration curves of the titratable sites.[11]

Furthermore, comparisons are made between dipeptide ligation in DdlB and depsipeptide ligation in VanA, one of the five essential enzymes involved in vancomycin resistance. DdlB and VanA share 45% sequence similarity (30% sequence identity) and are considered highly homologous. In various vancomycin-resistant strains of enterococci, VanA promotes the formation of the depsipeptide D-alanine-D-lactate (D-Ala-D-lac). D-Ala-D-lac is then incorporated into the disaccharide pentapeptide units in place of D-Ala-D-Ala. By replacing the amide bond with an ester bond, a hydrogen bond donor (NH) is exchanged for a hydrogen bond acceptor (O). This results in a 1000-fold reduction of binding for vanco-

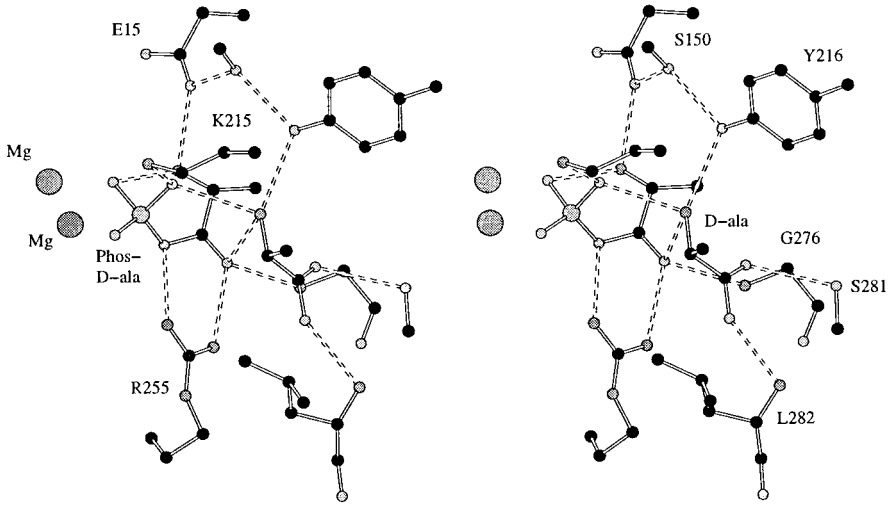

Figure 3. Stereoview of the active site obtained after replacing the phosphinophosphate inhibitor with phos-D-Ala$_1$ and D-Ala$_2$, adding hydrogens to the protein, and minimizing the structure. However, for clarity, the hydrogens are not shown in this figure.

mycin to the ends of the peptidoglycan units of enterococci.[1,2] Normally, vancomycin binds to the D-Ala-D-Ala tail of those units, prevents their cross-linking, and weakens the cell wall. With antibiotic-resistant strains of bacteria becoming more common and increasingly dangerous, new routes to therapeutic treatment are necessary. Dipeptide ligases are a potential system to be exploited, and the related depsipeptide ligases are also a target to restore vancomycin susceptibility to resistant bacterial strains.

Calculating the Titration Curves and pK_a Shifts

More complete details regarding the setup of the system and protocol of the calculations are given in the Computational Details section, but a brief account is required before discussing the results. The CHARMm 23.2 program[12] with the CHARMM all-atom force field[13] was used to create a computational model of the enzymatic system based on the crystal structure. Structures and partial charge parameters for phos-D-Ala$_1$ and D-Ala$_2$ were supplemented from ab initio molecular orbital calculations at the RHF/6-31+G* level. The phosphinophosphate transition-state mimic occupying the active site of DdlB in the crystal structure was replaced by the ligands, and the system was allowed to relax for 1000 steps of steepest-decent minimization. All side chains were modeled in their neutral states; this was done so that the protein and ligands did not minimize to a configuration that inherently promoted the zwitterionic states of the ligands. Although the ionization sites were modeled as neutral and there were no explicit water molecules used in the minimizations, the resulting interactions between the ligands and the active site parallel those in the crystal structure (see Figure 3). For calculating the titration curves, solvent was represented with a high-dielectric region, and the protein interior was modeled as a low-dielectric region with each atom as a fixed partial-charge site. To match experimental conditions, the ionic strength of the solvent was represented as 150 mM and the temperature was 310 K.[7]

pK_a shifts were calculated for all ionizable groups of the protein, cofactor, and ligands. The method has been well described previously, and the reader is pointed to the references for a detailed mathematic derivation.[11] It is known that protein environments can significantly shift the pK_a's of ligands and titratable side chains of various residues. The shifts result primarily from the electrostatic environment of the protein altering the stability of the charged state of the ionizable site. The pK_a shift can be calculated by comparing the free energy change for titrating the ionizable site in the protein to the free energy change of the same process in aqueous solution; the relative free energy change between the environments, $\Delta\Delta G$, is related to the pK_a shift as follows:

$$\Delta \mathrm{p}K_a = \frac{-(\pm 1)\Delta\Delta G}{RT \ln 10} \qquad (1)$$

In this study, the titration of the ionizable sites is modeled as the simple addition of a +1 or −1 charge on a specific atom at the center of the group. The electrostatic component of the free energy change corresponding to the introduction of this unit charge has two contributions: the electrostatic interaction between the unit charge and the fixed partial charges within the protein environment and $^1/_2$ the electrostatic interaction with the dielectric continuum regions (Born-type interactions). The electrostatic potential is calculated by solving the Poisson−Boltzmann equation, in this case, through a finite-difference method employed in the UHBD program, version 5.1.[14]

This only gives the ΔpK_a for a single site in the protein environment without the other sites being ionized. The titration curves are determined through a "clustering method" which calculates the ionization fraction based on the Boltzmann weighting of all multiple ionization states calculated with the pH, ΔpK_a, and electrostatic interactions of all the titratable sites.[11] The final pK_a's reported in this study are taken from the p$K_{1/2}$ of those titration curves.

Results

The calculated pK_a's of the ionizable groups are given in Table 1. The standard protocol for the ionization of tyrosine side chains is to treat the hydroxyl group as a proton donor, but for Y216 we are also interested in its

Table 1. Calculated pK_a's and Proton Occupancies at pH 7.5 and 9.0[a]

		charge				charge	
group	pK_a	pH 7.5	pH 9.0	group	pK_a	pH 7.5	pH 9.0
C-ter	5.9	−0.937	−0.998	Glu15	−2.8	−0.999	−1
				Glu17	4.0	−0.999	−1
Asp3	3.0	−1	−1	Glu32	4.5	−0.998	−1
Asp36	2.8	−1	−1	Glu44	4.8	−0.997	−1
Asp41	2.2	−1	−1	Glu68	−0.4	−0.999	−1
Asp46	3.7	−1	−1	Glu77	4.4	−0.996	−1
Asp69	2.2	−1	−1	Glu121	4.6	−0.997	−1
Asp96	0.9	−1	−1	Glu123	3.7	−1	−1
Asp128	2.9	−1	−1	Glu133	4.7	−0.998	−1
Asp165	3.7	−1	−1	Glu148	3.0	−0.991	−1
Asp174	0.3	−1	−1	Glu160	4.1	−0.999	−1
Asp211	3.2	−0.998	−1	Glu175	4.2	−0.998	−1
Asp219	3.7	−0.999	−1	Glu176	2.8	−0.999	−1
Asp257	−1.5	−1	−1	Glu180	0.3	−1	−1
Asp261	2.8	−1	−1	Glu187	3.6	−0.997	−1
Asp263	3.5	−1	−1	Glu195	4.3	−0.998	−1
Asp306	4.1	−0.971	−0.999	Glu196	4.1	−0.999	−1
				Glu213	5.0	−0.993	−1
His63	3.2	0.002	0	Glu220	4.1	−0.999	−1
His173	6.6	0.124	0.005	Glu230	4.2	−0.999	−1
His280	7.8	0.652	0.059	Glu234	4.1	−0.999	−1
				Glu270	−5.9	−1	−1
N-ter	7.7	0.591	0.052	Glu303	4.6	−0.997	−1
Cys225	10.7	−0.001	−0.028	Lys4	10.1	0.994	0.918
Cys250	10.8	−0.001	−0.033	Lys43	10.6	0.999	0.972
				Lys51	11.2	1	0.992
Tyr38	11.8	0	−0.006	Lys57	12.0	1	0.998
Tyr83	16.4	0	0	Lys97	21.0	1	1
Tyr210	18.1	0	−0.001	Lys101	13.4	1	0.999
Tyr212	11.2	−0.001	−0.013	Lys124	10.9	1	0.987
Tyr216[b]	18.9	0	−0.001	Lys129	11.7	1	0.998
Tyr223	14.8	0	0	Lys144	17.3	1	1
Tyr267	12.4	0	−0.002	Lys156	10.6	0.999	0.973
				Lys181	12.1	1	0.998
Arg16	13.8	1	1	Lys215	17.9	1	0.999
Arg31	13.6	1	1	Lys243	10.5	0.999	0.965
Arg65	15.9	1	1	Lys251	15.0	1	1
Arg99	13.8	1	1				
Arg119	13.5	1	1	ADP	4.8	−0.981	−0.999
Arg147	14.4	1	1				
Arg168	13.0	1	1	phos-D-Ala$_1$ (N)	11.6	0.998	0.974
Arg202	13.2	1	1	phos-D-Ala$_1$ (OP)	−17.9	−1	−1
Arg255	19.4	1	1	phos-D-Ala$_1$ (OP)	−10.6	−1	−1
Arg288	12.6	1	0.999				
Arg300	13.8	1	1	D-Ala$_2$ (N)	15.4	0.999	0.989
				D-Ala$_2$ (COO)	−6.4	−1	−1
charge at pH 7.5 = −12.5[c]							
charge at pH 9.0 = −14.2[c]							

[a] Proton occupancies are given as partial charges for the groups. [b] Note that for this table Y216 is modeled as a proton donor. [c] Final charges reflect the contributions of the two magnesium ions and the base charge of −2 for the model of ADP.

Table 2. Minor Differences in the Calculated pK_a's as a Result of the Description of Y216

Y216 as proton donor R-OH + H_2O ⇄ R-O^- + H_3O^+		Y216 as proton acceptor R-OH + H_2O ⇄ R-OH_2^+ + HO^-	
group	pK_a	group	pK_a
Lys101	13.4	Lys101	13.5
Tyr216	18.9	Tyr216	−21.1
Tyr223	14.8	Tyr223	14.9
Arg255	19.4	Arg255	20.0
D-Ala$_2$ (N)	15.4	D-Ala$_2$ (N)	15.1

role as a potential proton acceptor for the deprotonation of D-Ala$_2$. A second series of calculations was performed where Y216 was modeled as a proton acceptor, and most of the pK_a's were unchanged. The residues that were affected were generally within close proximity of Y216; those results are given in Table 2. In both tables, the proton occupancies are presented as fractional net charges at typical pH's used in experimental studies of DdlB and its mutants.

Titration curves were calculated for each ionizable site in the entire protein. Most sites yielded typical titration curves; examples are given in Figure 4. Unusual titration curves that were slightly elongated or had shoulders were obtained for only a few residues. These deformations occurred in extreme pH ranges, below 3 or over 10 pK_a units, where the titration curves are only speculative since the crystal structure would not accurately represent the protein structure under those conditions. The only exception was D306, the C-terminus of DdlB, where cooperativity was seen for the deprotonation of the two acids. The two acids of D306 behave like one site with two ionization transitions rather than two independent sites. A previous study by Bashford and Gerwert involved very similar calculations

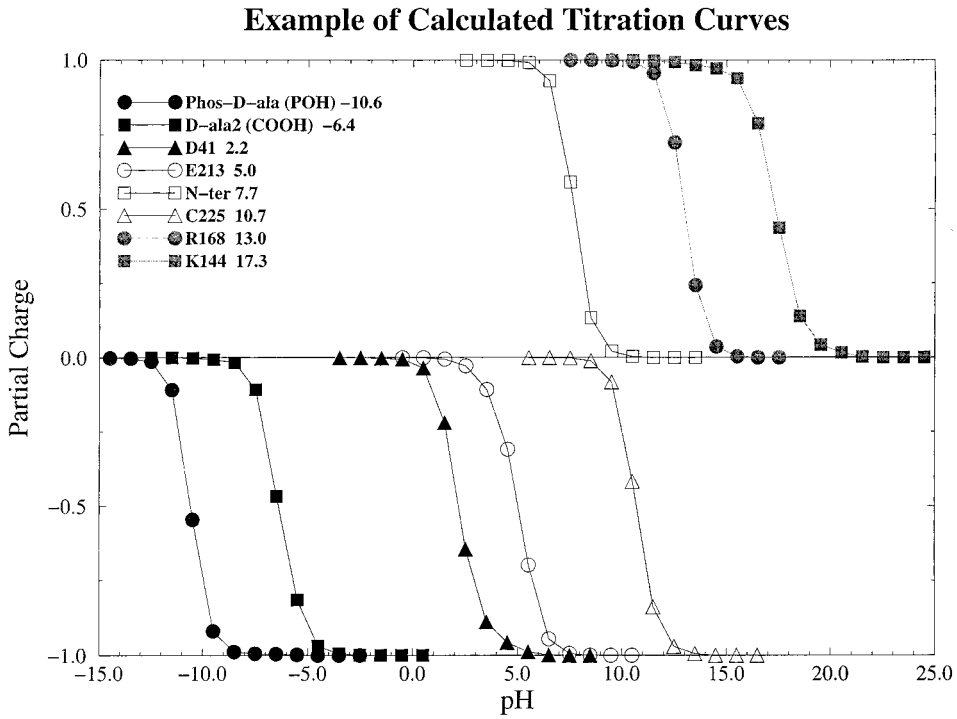

Figure 4. Most titration curves were calculated to be simple sigmoidal plots such as those shown here. Titration curves in the extreme pH are speculative, as one would expect dissociation of the ligands and/or rearrangement of the protein.

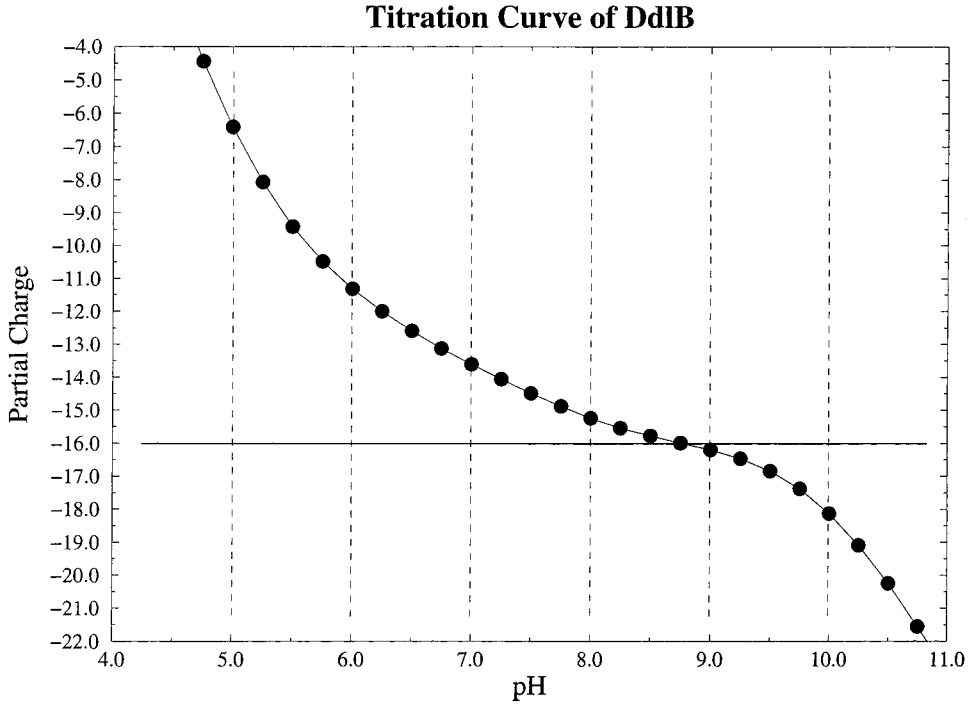

Figure 5. Titration curve for the entire DdlB system. The partial charges do not reflect the charges of the magnesium ions or the base charge of −2 for ADP. The horizontal line shows the inflection point of the system. The total charge of the system is most stable in the pH range of 8.0−9.5.

to determine the pK_a's and titration curves of the ionizable sites within bacteriorhodopsin.[15] Similar titration characteristics with a range of cooperativity were seen for acidic side chains. While the titration behavior suggested for the two acid groups of D306 is interesting to note, the C-terminus is on the surface of DdlB, too far from the active site to significantly contribute to shifting the pK_a's of the ligands. The titration curves for D306 are presented in Supporting Information.

With 83 individual sites, presenting each would be rather lengthy, but added together, they provide the titration curve of the entire DdlB system, Figure 5. The titration of the system is smooth and gradual over the pH range of 6.25−9.5 (cumulative charge of the ionizable sites varies from −12 to −17). Over this range, the primary contributions to the changing ionization of the system are the termini and the side chains of H173, H280, and K4. Each of these sites is on the surface of the protein, away from the active site. The inflection

point for the system is at pH 8.75 where the total charge of all ionizable groups is −16; addition of the charges from the magnesium ions and ADP makes the total system charge equal to −14. This point of stability happens to be in good agreement with the optimal pH of the system, 9.0, when the largest populations of D-Ala_2 would be present with a free-base amine in the active site without the lysines becoming deprotonated and destabilizing the protein structure. Note that the partial charge of the amine of D-Ala_2 is 0.989 at pH 9.0. This indicates that D-Ala_2 is in the free-base form 1.1% of the time that it occupies the second active site.

Discussion

Charge States within the Active Site. All lysine and arginine side chains are protonated in the active site over the range of pH's used in experimental studies of DdlB (pH 6−9.5). Acidic side chains in the active site are deprotonated over the same range. Such results were anticipated.

When phos-D-Ala_1 and D-Ala_2 are bound, H63 is neutral and ADP is in its trianionic charge state. The protein−ligand environment increases the acidity of H63 by approximately 3 pK_a units. The pK_a of ADP is also shifted 1.6 pK_a units more acidic. These shifts are due to the proximity of positive charges: the magnesium ions for ADP and the amine of phos-D-Ala_1 for H63. The current study cannot address whether the ionization states of H63 and ATP/ADP change upon binding the first or second D-Ala. Though the calculations could be repeated with the second or both D-alanine absent, it is not clear whether the configuration of the protein from the crystal structure is appropriate. Because of the buried nature of the active site of DdlB, the binding process must involve displacement of some residues (flexibility in the ω-loop, residues 206−220, has been suggested).[6,7,10] For the crystal structure, the active site was rigidified through cocrystallization with a transition-state mimic occupying both D-Ala binding sites;[6] an unoccupied active site may have very different conformations of the side chains and possibly movement of the ω-loop.

The primary goal of these calculations is to determine the most likely ionization states of the ligands, particularly D-Ala_2. We find that the active site of DdlB promotes the fully ionized forms of both phos-D-Ala_1 and D-Ala_2, more so than in aqueous solution. The amine of phos-D-Ala_1 is shifted 1.3 pK_a units more alkaline, and the phosphoester is significantly shifted more acidic because of its Coulombic interaction with the magnesium ions. The amine of D-Ala_2 is shifted 5.6 pK_a units more alkaline, and the carboxylic acid is shifted 8.7 pK_a units more acidic. The titration curve for the amine of D-Ala_2 indicates that the zwitterionic form dominates under experimental conditions with the free-base form present at 0.1% at pH 7.5 and 1.1% at pH 9.0.

Implications for VanA and Depsipeptide Ligation. As mentioned earlier, VanA is the depsipeptide ligase that catalyzes the formation of D-Ala-D-lac.[1,2] The sequence alignment of VanA and DdlB reveals that the active site is highly conserved—only three residues differ.[5,6] Y216 is replaced by a lysine, L282 is replaced by an arginine, and K215 is replaced by a glutamate. It has been proposed that the arginine at position 282 and the glutamate at position 215 could form a salt bridge and add to stabilizing the ω-loop.[6] The lysine at position 216 is considered crucial to the change in function between VanA and DdlB. Based on the proposal that D-Ala_2 binds as an anion with the amine in its free-base form, it was suggested that the lysine at position 216 alters the catalysis in VanA.[16] Having a lysine adjacent to the second ligand was proposed to promote the alkoxide of D-lac. An alkoxide is a stronger nucleophile than an amine, which results in better catalysis.

However, it is important to point out that VanA catalyzes both the depsipeptide ligation of D-Ala-D-lac and the dipeptide ligation of D-Ala-D-Ala. In fact, VanA actually catalyzes the dipeptide formation more efficiently than the depsipeptide ligation.[10] k_{cat} for D-Ala-D-Ala formation is 940 min^{-1} at pH 7.5; k_{cat} for D-Ala-D-lac ligation is 45 min^{-1} under the same conditions. VanA is a depsipeptide ligase because of a change in binding affinity, not a change in catalysis. This is evident by comparing the dissociation constants of D-Ala and D-lac in the second binding site of VanA at pH 7.5. K_{m2} for D-Ala is ≫100 mM, resulting in a k_{cat}/K_{m2} of 1.7 mM^{-1} min^{-1}. K_{m2} for D-lac is 0.88 mM, resulting in a k_{cat}/K_{m2} value of 51 mM^{-1} min^{-1}. As the pH is increased over a range from 6.4 to 8.3, VanA continues to preferentially bind D-lac but catalyze D-Ala-D-Ala ligation more efficiently.[10] We propose that the altered binding affinity is due to the differing charge characteristics of the anionic D-lac and the zwitterionic D-Ala. D-Ala_2 may bind more poorly because of Coulombic repulsion between its ammonium and the adjacent lysine at position 216. This is in agreement with the original report of the crystal structure,[6] but more recent publications have promoted the idea that D-Ala_2 is an anion like D-lac.[7,10] If both D-Ala_2 and D-lac were anions, there would be little explanation to the preferential binding seen for VanA.

The Deprotonation Step. Once we conclude that D-Ala_2 binds within the active site as a zwitterion, the question becomes, "how is it deprotonated?" The amine must be in its free-base form for the reaction to proceed. After excluding Y216 as a proton acceptor (see Table 2), there are still several possible catalytic bases in the active site for the deprotonation step. The delocalized negative charges of the phosphoester made it a definite possibility,[16] but their proximity to the magnesium makes the sites *very* acidic with pK_a's of −17.9 and −10.6. The least acidic site (pK_a of 4.8) is the titration site on the β-phosphate of ADP. This would make ADP the most likely candidate except that ADP and D-Ala_2 are not linked by any set of hydrogen bonds. Of course, the current study cannot address the role of individual water molecules, either as the catalytic base or as a hydrogen-bonding network to other sites. The calculations presented here described the solvent as a high-dielectric continuum, but studies that include explicit water molecules are in progress. This leaves two sites, though both are quite acidic, as the most probable participants in the deprotonation of D-Ala_2: E15 and the carboxylic acid of D-Ala_2. E15 is the less acidic of the two sites, pK_a of −2.8, making it the more likely candidate. It is also part of a hydrogen-bonding triad that is thought to stabilize the flexible ω-loop over the active site; see Figure 1.[6,7] It would be quite interesting

if this triad played more than a structural role. The ammonium of D-Ala$_2$ donates a hydrogen bond to the hydroxyl of Y216 that, in turn, donates a hydrogen bond to the hydroxyl oxygen of S150 that donates a hydrogen bond to E15. This creates a chain of hydrogen bonds to connect D-Ala$_2$ to E15 and may allow the proton to shuttle to E15.

Arguments can also be made against E15 as the recipient of the proton in the deprotonation step. The hydrogen would be transferred through Y216, and this is unlikely. An additional argument against E15 as the catalytic base is that after the proton transfer, E15 will be protonated at the oxygen that accepts a hydrogen bond from the ammonium of phos-D-Ala$_1$. No hydrogen bonds will necessarily be lost, but the charge complement will be. It could be argued that this may facilitate product release from the active site, but it is not clear that there is an advantage to reducing the binding affinity of phos-D-Ala$_1$ prior to the catalysis of the dipeptide bond formation.

As mentioned earlier, there is only one functional group of the ligands that is not bound to the active site through charge complementarity. This group is the carboxylate of D-Ala$_2$. Quantum mechanics calculations of the zwitterionic form of alanine yield a distance between the oxygen of the carboxylate and the hydrogen of the ammonium of 1.64 Å and an N−H···O angle of 129.4°.[17] This fits the geometry requirements of a hydrogen bond. A proton transfer through this internal hydrogen bond could create a free-base amine and a trans rotomer of the carboxylic acid without eliminating other hydrogen bonds or complementary charge interactions within the active site. Of course, this study has already shown that the protein environment promotes the zwitterionic form of D-Ala$_2$, making this proton transfer more difficult. Ab initio molecular orbital calculations are required to more accurately address the issue of deprotonation, particularly an internal proton transfer. Such calculations are currently in progress.

Conclusion

The present calculations provide evidence that D-Ala$_2$ binds as a zwitterion in the active site of DdlB. The pK_a's of the ionizable groups indicate that the deprotonation of D-Ala$_2$ may proceed via an internal proton transfer, but it is also possible that the proton could be transferred to E15 or ADP through some chain of hydrogen bonds from the protein and/or water molecules. Though it is true that the free-base form of D-Ala$_2$ is the catalytically relevant species for dipeptide ligation, it is important to consider its dominant state in the active site. The preference for binding the zwitterionic form is very relevant for the design of inhibitors and the issue of dipeptide versus depsipeptide ligation in the vancomycin-resistance cascade.

We propose that VanA is a depsipeptide ligase because of altered binding specificity as a result of the different charge characteristics of the zwitterionic D-Ala$_2$ and the anionic D-lac. Information regarding the binding of substrates in DdlB and VanA is important for targeting dipeptide and depsipeptide ligases in the development of new antibiotics. There is additional information available for single-site mutants of DdlB, which more closely resemble VanA. Some of these mutants are depsipeptide ligases at low pH. We have initiated calculations to address the changes in binding and activity for these mutants.

Computational Details

Calculations began with structural optimizations of phos-D-Ala$_1$ and D-Ala$_2$ with all functionalities in their neutral states. The Gaussian94 program was used to conduct ab initio molecular orbital calculations at the RHF/6-31+G* level.[18] The structures were determined with energy minimizations, and the atom-centered partial charges were determined by fitting to the electrostatic potential with the CHELPG procedure as implemented in Gaussian94.

The computational model of the enzymatic system was based on the crystal structure. The RHF/6-31+G*-optimized structures were overlaid with the appropriate, non-hydrogen atoms of the phosphinophosphate transition-state mimic which was cocrystallized with DdlB. Partial charges for phos-D-Ala$_1$ and D-Ala$_2$ were taken from the ab initio calculations while Lennard−Jones and internal force-field parameters were taken from the CHARMM all-atom force field.[13] It should be noted that the dihedral angles of the phosphoester of phos-D-Ala$_1$ were held at their values determined from the RHF/6-31+G*-determined structures because there were no appropriate dihedral angle parameters available. The CHARMm 23.2 program[12] with the CHARMM all-atom force field[13] was used to add hydrogens, including nonpolar hydrogens, to the crystal structure of the protein, and the system was allowed to relax for 1000 steps of steepest-decent minimization. During the minimization, the background dielectric was set to 4.0 and the cutoffs were set large enough so that no intra- or intermolecular interactions were neglected. All hydrogens were allowed to optimize as well as the D-Ala ligands and all atoms within 11 Å of the ligand (except for the protein backbone).

Recalling that ionization is modeled as the addition of a unit charge to the neutral form of each site, the titratable groups of the protein were initially modeled in their neutral states: i.e., amines were in free-base form, carboxylates were neutral carboxylic acids, tyrosines had standard hydroxyl groups, etc. On the basis of their environments in the crystal structure, all three histidines were modeled with hydrogens on Nδ and titratable at Nϵ. ADP was modeled as a single titration site with two phosphate hydroxyls deprotonated and the third hydroxyl ionizable. This titration site was at the β-phosphate oxygen that was not adjacent to the two magnesium ions in the active site; it was assigned an initial pK_a of 6.4.[9] The ionizable groups were given initial pK_a's of 3.8 for the C-terminus, 4.0 for Asp, 4.4 for Glu, 6.3 for His, 7.5 for the N-terminus, 8.3 for Cys, 9.6 for Tyr, 10.4 for Lys, and 12.0 for Arg.[19,20] The initial pK_a's for phos-D-Ala$_1$ were 10.3 for the amine and 4.8 and 1.2 for the phosphate group.[21] The initial pK_a's for D-Ala$_2$ were 9.8 and 2.3 for the amine and carboxylic acid, respectively.[9] Charges of +1 were added at the nitrogens of the amines, Cζ of the arginines, and Nϵ of the histidines to model protonation. Deprotonation was modeled by adding −1 charges to the central carbons of the carboxylic acids, oxygens of the hydroxyl groups, sulfurs of the thiol groups, and the appropriate oxygens of the phosphate groups. When solving the finite-difference Poisson−Boltzmann equation using the UHBD program,[14] "focusing" grids with spacings of 2.5, 1.2, 0.75, and 0.25 Å were used. Dielectric boundary smoothing was employed, and an ion-exclusion layer around the immediate surface of the protein (the Stern layer) was defined with a 2.0-Å probe. The solvent dielectric was 80 and that of the protein interior was 20. Again, the ionic strength of the solvent was 150 mM and the temperature was 310 K.

The choice of a protein dielectric of 20 may appear to be too high given the frequent use of 2 or 4. In the development of the protocol for these pK_a calculations, Antosiewicz, McCammon, and Gilson had found that a value of 20 produced the closest agreement with experiment.[19,20] There are several possible reasons. This simplified method of adding a unit

charge to a single atom site may be a bit crude and require more screening between ionization sites. Also, the positions of the atoms are held fixed during the calculations, so the dipoles and hydrogen bonds cannot respond to the electrostatic field. The higher dielectric may compensate for neglecting this type of polarization within the protein environment. The available force fields have been developed for simulations with explicit solvent models; adjusting the dielectric may be necessary to provide optimum performance when used with continuum solvent. Finally, choices in the setup of the calculations were made to err to the conservative, in this case, to prefer the free-base form of D-Ala_2. DdlB has a large negative charge throughout the experimental pH range; if a low dielectric had been used for the protein, the internal environment would have little electrostatic dampening and would be expected to strongly promote the protonated forms of the amines of phos-D-Ala_1 and D-Ala_2.

To address the possibility of Y216 acting as the catalytic base during the binding and/or ligation, a second calculation was performed with Y216 modeled as a proton acceptor rather than the standard of a proton donor. The hydroxyl oxygen was the site for the addition of a +1 charge with an initial pK_a of −6.7.[22] All other protocols were maintained during the second calculation.

Acknowledgment. We would like to thank Drs. Jan Antosiewicz and Michael Gilson for the use of their programs and very helpful discussions. We also thank Prof. James Knox for providing the crystal structure of DdlB prior to its release in the Protein Data Bank. H.A.C. is grateful to the American Cancer Society for a Postdoctoral Fellowship (No. PF-4427) and also appreciates the opportunity to participate in the La Jolla Interfaces in Science Training Program that is supported through the Burroughs−Wellcome fund. This project is supported in part by NIH Grants GM31749 and GM56553. We also thank the San Diego Supercomputer Center for generous grants of computer time.

Supporting Information Available: RHF/6-31+G*-optimized structures of phos-D-Ala_1 and D-Ala_2 with their atom-centered partial charges and titration curves for D306. This material is available free of charge via the Internet at http://pubs.acs.org.

Appendix

In the experimental studies,[7,10] the kinetic analysis for the dipeptide ligation was solved under the assumption that the first and second ligands were identical.

$$E + 2S \overset{K_{m1}}{\rightleftharpoons} ES + S \overset{K_{m2}}{\rightleftharpoons} ES^2 \xrightarrow{k_{cat}} E + P \qquad (2)$$

Assuming a steady-state approximation, the following relationship is obtained.[7,10]

$$\frac{1}{V} = \frac{1}{V_{max}} + \frac{K_{m2}}{V_{max}}\frac{1}{[S]} + \frac{K_{m1}K_{m2}}{V_{max}}\frac{1}{[S]^2} \qquad (3)$$

The experimental values of the kinetic parameters were obtained by fitting data to eq 3.

Let us consider the case that D-Ala_2 binds as an anion with a free-base amine and that D-Ala_1 and D-Ala_2 represent the only two forms of D-alanine available in solution (the populations of the neutral and cationic forms will be small in comparison to the anionic and zwitterionic forms in the experimental pH range). The following equations hold true where S_1 denotes the zwitterionic D-Ala_1 and S_2 is the anionic D-Ala_2.[10]

$$E + S_1 + S_2 \overset{K'_{m1}}{\rightleftharpoons} ES_1 + S_2 \overset{K'_{m2}}{\rightleftharpoons} ES_1S_2 \xrightarrow{k_{cat}} E + P \qquad (4)$$

$$\frac{1}{V} = \frac{1}{V_{max}} + \frac{K'_{m2}}{V_{max}}\frac{1}{[S_2]} + \frac{K'_{m1}K'_{m2}}{V_{max}}\frac{1}{[S_1]}\frac{1}{[S_2]} \qquad (5)$$

Equation 4 and 5 were used for the analysis of depsipeptide, D-Ala-D-lac, formation in the experimental studies.[10] In the case of D-Ala_1 and D-Ala_2, the concentrations of S_1 and S_2 are related through the Henderson−Hasselbalch equation.

$$[S_2]/[S_1] = 10^{pH-pK_a} \qquad (6)$$

Since the total concentration of D-alanine available in solution is equal to the sum of the concentrations of zwitterionic and free-base forms ($[S] = [S_1] + [S_2]$), it readily follows that

$$[S_1] = [S]/(1 + 10^{pH-pK_a}) \qquad (7)$$

$$[S_2] = [S]/(1 + 10^{pK_a-pH}) \qquad (8)$$

Substituting the values from eqs 7 and 8 into eq 5, we obtain eq 9.

$$\frac{1}{V} = \frac{1}{V_{max}} + \frac{K'_{m2}(1 + 10^{pK_a-pH})}{V_{max}}\frac{1}{[S]} + \frac{K'_{m1}(1 + 10^{pH-pK_a})K'_{m2}(1 + 10^{pK_a-pH})}{V_{max}}\frac{1}{[S]^2} \qquad (9)$$

Comparing eq 9 to eq 3 used to fit the experimental data, the pH dependence of K_{m1} and K_{m2} is obvious.

$$K_{m2} = K'_{m2}(1 + 10^{pK_a-pH}) \qquad (10)$$

$$K_{m1} = K'_{m1}(1 + 10^{pH-pK_a}) \qquad (11)$$

K'_{m2} and K'_{m1} are binding constants which are independent of the concentration of the zwitterionic and anionic D-alanine in solution. The pH effects on K'_{m2} and K'_{m1} should come only from changes in the protein environment, but the pH effects on K_{m2} and K_{m1} should come primarily from changes in the concentrations of the two forms of D-alanine with the changes in the protein being secondary. Note that at a pH equal to the pK_a of the amine (9.8), K_{m2} would be twice the value of K'_{m2}, reflecting that the total concentration of D-alanine in solution (which is the value used to fit K_{m2}) is twice the concentration of the anionic form of D-Ala_2 at pH 9.8.

A graph of $\log(1/K_{m2})$ versus pH should exhibit a near linear relationship with a slope of approximately 1 for pH's below 10. Therefore, one would expect an increase in $\log(1/K_{m2})$ of 3 log units over the pH range of 6.0−9.5; a similar increase would be seen for $\log(k_{cat}/K_{m2})$. One would also anticipate a 2100-fold decrease in K_{m2} over the same pH range, as the scaling factor in parentheses in eq 10 would decrease from 6311 to 3. There would be very little increase in K_{m1} as the scaling factor in eq 11 would change from 1.0002 to 1.501.

The experimentally determined kinetic parameters were reported for pH's of 6.0, 7.5, and 9.2.[10] *If D-Ala_2 were bound in the free-base form, there should be a 1300-fold decrease in K_{m2} in going from pH 6.0 to pH 9.2.* In the experimental studies, the variation reported for K_{m2} is only a 7-fold decrease;[10] the effect of pH on K_{m2} appears to be 3 orders of magnitude too small to agree with the hypothesis that the anionic form of D-Ala_2 binds to the enzyme. The minor decrease seen in K_{m2} points to the concentration of the bound form of D-Ala_2 being relatively constant over the experimental pH range. Therefore, we conclude that D-Ala_2 is the zwitterionic species, and any increase or decrease in the experimental kinetic parameters results from changes in the protein environment with pH as mentioned in the discussion of K'_{m1} and K'_{m2}.

References

(1) Walsh, C. T.; Fisher, S. L.; Park, I.-S.; Prahalad, M.; Wu, Z. Bacterial resistance to vancomycin: Five genes and one missing hydrogen bond tell the story. *Chem. Biol.* **1996**, *3*, 21−28.

(2) Arthur, M.; Reynolds, P. E.; Depardieu, F.; Evers, S.; Dutka-Malen, S.; Quintiliani, R.; Courvalin, P. Mechanisms of glycopeptide resistance in Enterococci. *J. Infect.* **1996**, *32*, 11−16.
(3) Park, J. T. The Murein Sacculus and Murein Synthesis. In *Escherichia coli and Salmonella typhimurium: Cellular and molecular biology*; Neidhardt, F. C., Ed.; American Society for Microbiology: Washington, DC, 1987; pp 23−30, 663−671.
(4) Georgopapadakou, N. H. New cell wall antibiotic targets. In *Antibiotic Inhibition of Bacterial Cell Surface Assembly and Function*; Actor, P., Daneo-Moore, L., Higgins, M. L., Salton, M. R. J., Shockman, G. D., Eds.; American Society for Microbiology: Washington, DC, 1988; pp 505−508.
(5) Evers, S.; Casadewall, B.; Charles, M.; Dutka-Malen, S.; Galimand, M.; Courvalin, P. Evolution of structure and substrate specificity in D-alanine: D-alanine ligases and related enzymes. *J. Mol. Evol.* **1996**, *42*, 706−712.
(6) Chang, F.; Moews, P. C.; Walsh, C. T.; Knox, J. R. Vancomycin resistance: Structure of D-alanine:D-alanine ligase at 2.3 Å resolution. *Science* **1994**, *266*, 439−443 (code 2DLN in Brookhaven PDB).
(7) Shi, Y.; Walsh, C. T. Active site mapping of *Escherichia coli* D-Ala-D-Ala ligase by structure-based mutagenesis. *Biochemistry* **1995**, *34*, 2768−2776.
(8) Neuhaus, F. C. The enzymatic synthesis of D-alanyl-D-alanine I. Purification and properties of D-alanyl-D-alanine synthetase. *J. Biol. Chem.* **1962**, *237*, 778−786.
(9) Martell, A. E.; Smith, R. M. *Critical Stability Constants*; Plenum Press: New York, 1974; Vol. 1−6.
(10) Park, I.-S.; Lin, C.-H.; Walsh, C. T. Gain of D-alanyl-D-lactate or D-lactyl-D-alanine synthetase activities in three active site mutants of *E. coli* D-alanyl-D-alanine ligase B. *Biochemistry* **1996**, *35*, 10464−10471.
(11) Gilson, M. K. Multiple-site titration and molecular modeling: Two rapid methods for computing energies and forces for ionizable groups in proteins. *PROTEINS* **1993**, *15*, 266−282.
(12) (a) *CHARMm 23.2, Quanta96;* Molecular Simulations Inc.: San Diego, CA, 1996. (b) Brooks, B. R.; Bruccoleri, R. E.; Olafson, B. D.; States, D. J.; Swaminathan, S.; Karplus, M. CHARMm: A program for macromolecular energy, minimization, and dynamics calculations. *J. Comput. Chem.* **1983**, *4*, 187−217.
(13) (a) Mackerell, A. D.; Wiórkiewicz-Kuczera, J.; Karplus, M. An all-atom empirical energy function for the simulations of nucleic acids. *J. Am. Chem. Soc.* **1995**, *117*, 11946−11975. (b) Pavelites, J. J.; Gao, J.; Bash, P. A.; Mackerell, A. D. A molecular mechanics force field for NAD^+, NADH, and the pyrophosphate groups of nucleotides. *J. Comput. Chem.* **1997**, *18*, 221−239.
(14) Madura, J. D.; Briggs, J. M.; Wade, R. C.; Davis, M. E.; Luty, B. A.; Ilin, A.; Antosiewicz, J.; Gilson, M. K.; Bagheri, B.; Scott, L. R.; McCammon, J. A. Electrostatics and diffusion of molecules in solution: Simulations with the University of Houston Brownian Dynamics program. *Comput. Phys. Commun.* **1995**, *91*, 57−95.
(15) Bashford, D.; Gerwert, K. Electrostatic calculations of the pK_a values of ionizable groups in bacteriorhodopsin. *J. Mol. Biol.* **1992**, *224*, 473−486.
(16) Ellsworth, B. A.; Tom, N. J.; Bartlett, P. A. Synthesis and evaluation of inhibitors of bacterial D-alanine:D-alanine ligases. *Chem. Biol.* **1996**, *3*, 37−44.
(17) Carlson, H. A.; McCammon, J. A. Unpublished results, 1998.
(18) Frisch, M. J.; Trucks, G. W.; Schlegel, H. B.; Gill, P. M. W.; Johnson, B. G.; Robb, M. A.; Cheeseman, J. R.; Keith, T.; Petersson, G. A.; Montgomery, J. A.; Raghavachari, K.; Al-Laham, M. A.; Zakrzewski, V. G.; Ortiz, J. V.; Foresman, J. B.; Cioslowski, J.; Stefanov, B. B.; Nanayakkara, A.; Challacombe, M.; Peng, C. Y.; Ayala, P. Y.; Chen, W.; Wong, M. W.; Andres, J. L.; Replogle, E. S.; Gomperts, R.; Martin, R. L.; Fox, D. J.; Binkley, J. S.; Defrees, D. J.; Baker, J.; Stewart, J. P.; Head-Gordon, M.; Gonzalez, C.; Pople, J. A. *Gaussian94, Revision E.2*; Gaussian, Inc.: Pittsburgh, PA, 1995.
(19) Antosiewicz, J.; McCammon, J. A.; Gilson, M. K. Prediction of pH-dependent properties of proteins. *J. Mol. Biol.* **1994**, *238*, 415−436.
(20) Antosiewicz, J.; McCammon, J. A.; Gilson, M. K. The determinants of pK_as in proteins. *Biochemistry* **1996**, *35*, 7819−7833.
(21) Estimated from the pK_a's of acyl phosphate (this reference) and the ΔpK_a between the amines of phosphoserine and serine (ref 9). Kluger, R.; Wasserstein, P.; Nakaoka, K. Factors controlling association of magnesium ion and acyl phosphates. *J. Am. Chem. Soc.* **1975**, *97*, 4298−4303.
(22) Streitwieser, A.; Heathcock, C. H. *Introduction to Organic Chemistry*, 2nd ed.; Macmillian Publishing: New York, 1981; Appendix IV.

JM980351C